Journal of Orthopaedic Translation 37 (2022) 12–22

Contents lists available at ScienceDirect

Journal of Orthopaedic Translation

journal homepage: www.journals.elsevier.com/journal-of-orthopaedic-translation

ECFC-derived exosomal THBS1 mediates angiogenesis and osteogenesis in distraction osteogenesis via the PI3K/AKT/ERK pathway

Fengchun Liao [a,b,c,d,1], Ziqi Liao [a,b,c,d,1], Tao Zhang [a,b,c,d,1], Weidong Jiang [a,b,c,d], Peiqi Zhu [a,b,c,d], Zhenchen Zhao [a,b,c,d], Henglei Shi [a,b,c,d], Dan Zhao [a,b,c,d], Nuo Zhou [a,b,c,d,**], Xuanping Huang [a,b,c,d,*]

[a] Department of Oral and Maxillofacial Surgery, College of Stomatology, Guangxi Medical University, 10 Shuangyong Road, Nanning, 530021, People's Republic of China
[b] Guangxi Clinical Research Center for Craniofacial Deformity, Nanning, 530021, People's Republic of China
[c] Guangxi Key Laboratory of Oral and Maxillofacial Rehabilitation and Reconstruction, Nanning, 530021, People's Republic of China
[d] Guangxi Key Laboratory of Oral and Maxillofacial Surgery Disease Treatment, Nanning, 530021, People's Republic of China

ARTICLE INFO

Keywords:
Endothelial colony-forming cell
Exosome
Distraction osteogenesis
Angiogenesis

ABSTRACT

Background: Distraction osteogenesis (DO) is a widely used bone regenerative technique. However, the DO process is slow, and the consolidation phase is long. Therefore, it is of great clinical significance to explore the mechanism of DO, and shorten its duration. Recent studies reported that stem cell exosomes may play an important role in promoting angiogenesis related to DO, but the mechanism remains unclear.

Methods: Canine endothelial colony-forming cells (ECFCs) were isolated and cultured, and the expression of THBS1 in canine ECFCs were inhibited using a lentiviral vector. The exosomes secreted by canine ECFCs were isolated and extracted, and the effect of exosomes on the angiogenic activity of Human umbilical vein endothelial cells (HUVECs) was detected by proliferation, migration, and tube formation experiments. WB and qRT-PCR were used to explore the effects and mechanisms of THBS1-mediated ECFC-Exos on HUVECs angiogenesis. Then, a mandibular distraction osteogenesis (MDO) model was established in adult male beagles, and exosomes were injected into the canine peripheral blood. Micro-CT, H&E, Masson, and IHC staining were used to explore the effects and mechanisms of THBS1-mediated ECFC-Exos on angiogenesis and osteogenesis in the DO area.

Results: ECFC-Exo accelerated HUVECs proliferation, migration and tube formation, and this ability was enhanced by inhibiting the expression of THBS1 in ECFC-Exo. Using Western blot-mediated detection, we demonstrated that inhibiting THBS1 expression in ECFCs-Exo activated PI3K, AKT, and ERK phosphorylation levels in HUVECs, which promoted VEGF and bFGF expressions. In the DO model of the canine mandible, ECFCs-Exo injected into the peripheral blood aggregated into the DO gap, thus promoting angiogenesis and bone formation in the DO tissue by reducing THBS1 expression in ECFC-Exo.

Conclusion: Our findings suggested that ECFC-Exos markedly enhances angiogenesis of endothelial cells, and promotes bone healing in canine MDO. Thus, THBS1 plays a crucial role in the ECFC-Exos-mediated regulation of canine MDO angiogenesis and bone remodeling.

The translational potential of this article: This study reveals that the angiogenic promotion via THBS1 suppression in ECFC-Exos may be a promising strategy for shortening the DO duration.

Abbreviations: DO, Distraction osteogenesis; ECFC, Canine endothelial colony-forming cell; HUVEC, Human umbilical vein endothelial cell; EPC, Endothelial progenitor cell; THBS1, Thrombospondin 1; eEPC, Early endothelial progenitor cell; MNCs, Mononuclear cells; TEM, Transmission electron microscope; siRNA, Small interfering RNA; MDO, Mandibular distraction osteogenesis; BV/TV, Bone volume to total volume ratio; Tb.N, Trabecular number; Tb.Th, Trabecular thickness; Tb.Sp, Trabecular separation; BMD, Bone mineral density; IHC, Histological and immunohistochemical.

* Corresponding author. Department of Oral and Maxillofacial Surgery, College of Stomatology, Guangxi Medical University, 10 Shuangyong Road, Nanning, 530021, People's Republic of China.

** Corresponding author. Department of Oral and Maxillofacial Surgery, College of Stomatology, Guangxi Medical University, 10 Shuangyong Road, Nanning, 530021, People's Republic of China.

E-mail addresses: zhounuo@gxmu.edu.cn (N. Zhou), huangxuanping@gxmu.edu.cn (X. Huang).

[1] These authors have contributed equally to this work.

https://doi.org/10.1016/j.jot.2022.08.004
Received 26 April 2022; Received in revised form 24 July 2022; Accepted 9 August 2022

1. Introduction

Distraction osteogenesis (DO) is a widely used bone regenerative technique. Its osteogenesis rate is 4–6 times that of a normal child development [1]. However, the DO process is slow, and the consolidation phase is long. Thus, it is inconvenient to patient life, and enhances complication risks. Therefore, it is of great clinical value to explore the mechanism of DO, and shorten its duration.

Blood vessels determine the local microenvironment in the skeletal system, and they play a crucial role in osteogenesis. Successful bone formation is highly dependent on neovascularization, and it involves a multi-layered and mutually responsive biological regulatory network that interlinks neovascularization and bone regeneration [2], which, is known as osteogenic-angiogenic coupling effect [3]. Unfortunately, inadequate blood supply during the consolidation phase can lead to multiple complications, including, nonunion and delayed union [4]. Therefore, it is of great significance to examine the DO-based angiogenesis mechanism to accelerate bone formation, and shorten DO duration.

Endothelial progenitor cells (EPCs) differentiate to form endothelial cells that are critical for angiogenesis. Circulating EPCs tend to increase during DO distraction and consolidation phases, and cultured and labeled EPCs are recruited to the distraction areas [5,6]. Endothelial colony-forming cells (ECFCs) or late EPCs, have strong proliferation ability, and form new blood vessels in vivo. They are often considered as "endothelial progenitor cells" because of their ability to produce endothelial cell progeny in a true sense [7]. ECFCs generally stimulate vascular repair through multiple mechanisms, such as, physical engraftment within neovascularization, paracrine release of pro-angiogenic mediators, secretion of exosomes, and synergy with other cells, and the activation of multiple mechanisms that synergistically promotes tissue revascularization [8]. Studies have shown that ECFCs secrete exosomes, which are key to their beneficial effects [9].

Exosomes are 30–150 nm diameter lipid bilayer membrane-based extracellular vesicles [10], and they can modulate function of target cells by transporting mRNA, microRNA, LncRNA or proteins [11,12]. Stem cell exosome therapy produces low immunogenicity, low rejection rates, specific targeting, circulatory stability, active crossing of biological barriers, which, lower risk of tumorigenicity and vascular thrombosis compared with stem cell therapy. Thus, this has become a research hotspot in a variety of fields, and is expected to replace stem cell therapy in the near future [13]. Studies clarified that entwined with angiocrine factors, osteoclast-derived exosomal-containing miRNAs play a critical role in angiogenesis–osteogenesis coupling essential in bone remodeling [14]. Zhang Y et al. [15] found that transplantation of uMSC-Exos markedly enhanced angiogenesis and bone healing processes in a rat model of femoral fracture. However, ECFC-Exos on DO angiogenesis and bone remodeling are rarely reported. Studies of remodeling are rarely reported, and the mechanism remains unclear.

Thrombospondin 1 (THBS1), or TSP-1, is the first native protein identified as an endogenous angiogenesis inhibitor [16]. The anti-angiogenic function of THBS1 is achieved through TSR interacting with the CLESH domain of CD36 and β-1 integrin, and the 3TSR interaction with α5β1 integrin inhibit endothelial cell migration in a PI3K-dependent manner [17]. The TSR of TSP-1 also interacts with the transmembranal protein tyrosine phosphatase CD148 expressed within endothelial cells, and peptides based on the TSR sequence can enhance CD148 activity against two substrates, EGFR and ERK1/2, thereby suppressing endothelial cell proliferation and angiogenesis [18]. Recently, a motif within the N-terminal domain of THBS1 was demonstrated to promote neovascularization by enhancing ECFCs chemotaxis and tubulogenesis [19]. In contrast, silencing THBS1 restores the angiogenic properties of ECFCs by enhancing AKT phosphorylation [20]. EPC-exosomes were also identified to deliver miR-21-5p, and suppress THBS1 expression to enhance endothelial cell repair [21]. Conversely, THBS1 overexpression in the secretome of early endothelial progenitor cells (eEPC) prevents angiogenesis of ECFC [22].

Therefore, we hypothesized that THBS1 is crucial for the ECFC-Exos-mediated angiogenesis activity. Hence, this study explored the impact of ECFC-exo-THBS1 on endothelial cell angiogenesis, and clarified its regulation of DO-mediated bone regeneration. It provides a new promising strategy for shortening the duration of DO.

2. Method

2.1. ECFC isolation and culture

ECFCs were isolated from canine peripheral blood samples (20 mL). Mononuclear cells (MNCs) were acquired via a canine peripheral blood mononuclear cell extraction kit (Solarbio, China) using density gradient fractionation, followed by re-suspension in complete medium (EGM-2; Lonza, USA) containing 10% FBS. They were next cultured on fibronectin-coated T25 cell dishes at 37 °C in a 5% CO_2 humid chamber. The ECFC phenotypes were assessed via flow cytometry, upon addition of antibodies against mouse CD34, CD45 CD105, and CD133 (Invitrogen, USA). Dil-ac-LDL uptake and FITC-UEA-1 binding assays were next performed with corresponding kits (Invitrogen, USA), following kit guidelines, to further examine the profiles of ECFC.

2.2. Isolation and identification of ECFC-exosomes

Upon reaching 80-90% confluency, the ECFCs medium was replaced with exosome-depleted FBS for 48h. The medium was then filtered using a 0.22 - μm filter, and centrifuged at 300g for 10 min at 4 °C. The supernatant was next collected and centrifuged at 2000g for 10 min at 4 °C, and the subsequent supernatant was again centrifuged at 10000g for 30 min at 4 °C. Next, upon removal of cellular debris and large vesicles, the supernatant was PBS-rinsed, followed by ultracentrifugation at 110,000×*g* for 90 min. The last step was repeated again. Then, the precipitate was resuspended in 4 ml PBS, and loaded into a 10-kD ultrafiltration tube. The mixture was centrifuged at 3000g for 30 min at 4 °C, and the volume was decreased to 200 μl. The resulting exosomes were stored at −80 °C.

We examined the exosome structure under a transmission electron microscope (TEM). The particle size and exosome concentration were analyzed via Flow NanoAnalyzer (Xiamen Fuliu Biological Technology Co., Ltd, China). Lastly, we analyzed the presence of particular exosome markers, namely, TSG101, CD63, CD81, and calxinnex using western blot.

2.3. HUVEC culture and selection of exosomes working concentration

Human umbilical vein endothelial cells (HUVECs) were purchased from BNBIO (Shang Hai, China). Cells were cultured in ECM medium (Sciencell, USA) at 37 °C, 5% CO2, with 95% humidity. In order to determine the optimal working concentration of exosomes, HUVECs were intervened by 5, 25 or 50 μg/ml ECFC-exosomes or vehicle control (PBS), then employed the CCK8, transwell and qRT-PCR assays to determine the impact of varying exosomes concentrations on HUVECs proliferation, migration, and angiogenesis ability. The optimal working concentration were selected for subsequent experimentations.

2.4. Exosome labelling and uptake assay

To assess exosome uptake by HUVEC, ECFC-Exos were labelled with PKH26 fluorescent dye (Sigma, USA), following kit protocols. Cells were exposed to PKH26 labeled exosomes for 8 h. The nucleus was stained with 4′,6-Diamidino-2-phenylindone (DAPI; Invitrogen, USA). Image capture was done via confocal laser microscope (Leica, **Germany**).

2.5. Lentiviral incorporation and transduction

The THBS1 small interfering RNAs (siRNAs), carrying a lentiviral vector with si-THBS1 (THBS1-shRNA), was designed and synthesized by the GeneChem Corporation (Shanghai, China). Here, we introduced negative control (transfected control eGFP lentivirus) as a control (Con-shRNA). ECFCs were transduced with an appropriate lentiviral vector (1×10^8 TU/mL) transfection. A 100 MOI was employed to determine suitable lentiviral vector dosages. We obtained THBS1- shRNA exosomes (shTHBS1-Exos group) and Con-shRNA exosomes (Con-Exos group) by extracting the cell culture medium from different groups of transfected-ECFCs.

2.6. Cell counting kit-8 (CCK8) assay

Cell proliferation was assessed via the CCK8-kit (Dojindo, Japan), as per kit directions. Cells were seeded in 96-well plates (2×10^3 cells/well), and the culture medium was refreshed every alternate day. HUVECs were treated with different groups of exosomes after adherence. At 0 h, 24 h, 48 h, 72 h respectively, medium from each well were replaced with 110 μL of the CCK-8 working solution (CCK-8: EGM culture medium, 1:10). Following 2 h incubation in the dark at 37 °C, an optical density of 450 nm (OD 450 nm) was detected using a spectrophotometer (Thermo Field, USA).

2.7. Transwell assay

Transwell chambers (Corning, USA) were employed for the assessment of cell migration in Transwell assays. The chambers were inserted into a 24-well plate, and cells (5×10^4 cells in 400 μL serum-free media) were introduced to the top chambers with different groups of exosomes, where they were grown for 24 h, following which 4% neutral-buffered formalin was utilized to fix cells that travelled to the bottom chamber. These cells next received hematoxyline staining (Solarbio, China), prior to imaging under a microscope (Nikon, Japan), and subsequent cell quantification.

2.8. Tube formation assay

We employed tube formation assay to determine the cellular angiogenic function. Matrigel (Corning, USA) was introduced onto a μ-slide angiogenesis plate (10 μL/well), prior to the placement of different groups of exosomes treated cells onto the plate (1.5×10^4 cells/well), followed by incubation for 12 h. Tube formation was then evaluated under a light microscope (Nikon, Japan), and quantification was done via the Image J software.

2.9. Quantitative real-time PCR analysis (qRT-PCR)

RNA was extracted from cells or callus tissue sample via TRIzol (Invitrogen, USA), following kit protocols. All cDNA synthesis was conducted via reverse transcription kit (Invitrogen, USA) for transcripts, and qRT-PCR was carried out with the QuantStudio-5 system (Applied Biosystems) using 2 × PowerUp SYBR Green Master Mix (Invitrogen, USA) and primers summarized in Table 1 β-actin and GAPDH were used as internal controls, and relative gene expression was computed using the $2-\Delta\Delta Ct$ formula.

2.10. Western blotting

We employed western blot assay to determine relevant protein content in cell lysates. Proteins from lysed cells were run on 10% SDS-PAGE, prior to transfer to PVDF membranes (Millipore, USA), which were then treated as follows: blocking in 5% non-fat milk in TBST at room temperature (RT) for 2 h, with subsequent exposure to primary antibodies against TSG101 (SBA, USA), CD63 (ABclonal, USA), CD81 (BIOSS, China), calxinnex (SAB, USA), THBS1 (Invitrogen, USA), VEGF (Invitrogen, USA), bFGF (BIOSS, China), PI3K (Bioworld, USA), p-PI3K (Bioworld, USA), AKT1 (Bioworld, USA), p-AKT1 (Bioworld, USA), ERK (Bioworld, USA), p-ERK (Bioworld, USA) and β-actin (Beyotime, China) diluted in TBST, and incubated overnight at 4 °C. And lastly, exposure to corresponding secondary antibody for 2 h at RT. Protein quantification was done with the Image J software.

Table 1
The primer sequences employed in our RT-qPCR reaction.

Gene	Primer (5′-3′)	Primer sequence
cfa-THBS1	Forward	GGCGCTCCTGTGATAGTCTC
	Reverse	TGGTTTCCCGTTCATCTGGG
cfa-β-actin	Forward	CCAAGGCCAACCGTGAGAA
	Reverse	GTCACCGGAGTCCATCACGA
VEGF	Forward	ATCGAGTACATCTTCAAGCCAT
	Reverse	GTGAGGTTTGATCCGCATAATC
TGF-β	Forward	AGCAACAATTCCTGGCGATACCTC
	Reverse	TCAACCACTGCCGCACAACTC
IGF	Forward	TGTCCTCCTCGCATCTCTTCTACC
	Reverse	CCTGTCTCCACACACGAACTGAAG
bFGF	Forward	CATCAAGCTACAACTTCAAGCA
	Reverse	CCGTAACACATTTAGAAGCCAG
GAPDH	Forward	ATGGCATGGACTGTGGTCAT
	Reverse	ATGGCATGGACTGTGGTCAT
cfa-VEGF	Forward	TCCACCATGCCAAGTGGT
	Reverse	CCATGAACTTCACCACTTCG
cfa-bFGF	Forward	AGAGAGCGTTGTGTCCATC
	Reverse	GCCCAGTTCGTTTCAGTGC
cfa-VE-cadherin	Forward	ACAACCCTCCAGAGTTCGCC
	Reverse	GCCGAGATTTGCACGACCAG

2.11. Animals

Thirty male Beagles (12-18 months old, weighing 10–15 kg) were obtained from the Experimental Animal Center of the Guangxi Medical University (Nanning, China). All animals were maintained in iron cases in a temperature-regulated environment (25 ± 3 °C, constant humidity) with open access to standard food and sterile water. All animal studies described herein were reviewed and approved by the Animal Care and Use Committee of Guangxi Medical University (No. 202012014).

2.12. Mandibular distraction osteogenesis (MDO) model establishment

Twenty-seven healthy adult male Beagles were arbitrarily separated into 3 populations: NS (intravenous (i.v.) administration of 4 ml normal saline, 2 ml each time, divided into two shots), Con-Exos (i.v. administration of 550 μg exosomes isolated from ECFCs incorporated with negative virus. The exosomes were resuspended in 4 ml normal saline, and separated into two shots), and shTHBS1-Exos (i.v. administration of 550 μg exosomes isolated from ECFCs incorporated with shTHBS1 lentivirus. The exosomes were resuspended in 4 ml normal saline, and separated into two shots). The dogs were intraperitoneally anesthetized by administering 0.1 mL/kg pentobarbital sodium and 2 mg/kg xylazine. The distractor (Cibei, China) was installed on the right mandible, and the disconnected line was adjusted on the mandibular first and second molars. Following 7 days of latency, we performed distraction at 1-mm/day in two 12-h steps for 7 days. Dogs were provided with an i.v. injection of normal saline or exosomes on days 1 and 4 of distraction. In addition, following surgery, the dogs received an intramuscular injection of cephalosporin and tramadol hydrochloride for 3 consecutive days. Following 7 days of distraction, 9 dogs were euthanized at a consolidation phase of 0 days, 7 days, and 28 days (DO14, DO21 and DO 42), and samples were collected for analyses.

To elucidate the significance of exosomes in filling the distraction gap following i.v. administration, three dogs were i.v. injected with PKH26-labeled ECFCs-Exos on days 1 and 4 after distraction. After 7 days of distraction, dogs were euthanized and samples were collected. We next

prepared frozen sections, and stained with DAPI. Image capture was done on a confocal laser microscope.

2.13. Bone phenotyping

The DO callus tissue samples were analyzed via micro-computed (Micro-CT) tomography (Hitachi, Japan). The DICOM format data of the DO42-day samples were employed for 3D reconstruction using the VGStudio MAX22 software (Bruker, Germany). The obtained parameters were analyzed in terms of bone volume to total volume ratio (BV/TV), trabecular number (Tb.N), trabecular thickness (Tb.Th), and trabecular separation (Tb.Sp). The bone mineral density (BMD) of the regenerated bone were analyzed using the Latheta V3.61B software (Hitachi, Japan).

2.14. Histological and immunohistochemical (IHC) analyses

The DO callus tissue specimen were fixed with 4% paraformaldehyde, then decalcified via employing a decalcification solution, embedded with paraffin, and sectioned (4-μm) with a rotary microtome (RM2255, Leica, Germany). This was followed by H&E, Masson, and IHC staining for the evaluation of regeneration ability via an inverted microscope. In terms of IHC staining, anti-OCN and rabbit anti-CD31 (Bioss, 1:100, Cat. bs-0195R) were employed for the detection of vascular and osteogenic bio-markers.

2.15. Statistical analysis

All data analyses were done via SPSS software (version 23.0), and are expressed as means ± standard deviations (x ± s). In terms of evaluating the homogeneity of variances, differences among groups were compared via ANOVA. In presence of non-homogenous variance, data were analyzed via the non-parametric Kruskal–Wallis rank sum test. $P < 0.05$ was set as the significance threshold. ($^{*}P < 0.05$, $^{**}P < 0.01$, $^{***}P < 0.001$).

3. Result

3.1. Identification of ECFCs and ECFC-Exos

ECFCs were obtained from canine peripheral blood as described above. ECFCs were identified via their morphology, tube formation capacity, surface markers, Dil-ac-LDL uptake, and FITC-UEA-1 binding assay. Isolated ECFCs exhibited a shuttle-like morphology after being in culture for 7 days, and formed cobblestone-like structures after 10 days in culture (Fig. 1a). Using tube formation assay, we confirmed that ECFCs were capable of tube formation (Fig. 1b). Our flow cytometric analysis revealed that the cells were highly positive for ECFC surface markers, including, CD34 and CD105, but negative for CD45 and CD133 (Fig. 1d). Additionally, the cultured cells incorporated Dil-Ac-LDL and interacted with Fitc-UEA-1 (Fig. 1c). TEM, NTA, and western blot analyses were next employed for the identification of ECFC-derived nanoparticles. The nanoparticles were either cup- or sphere-shaped, with a mean diameter of 104.48 ± 44.26 nm, and a mean particle concentration of 4.34E+11 particles/ml. Based on our western blot assay, the nanoparticles contained enriched proteins like CD63, CD81, and TSG101, but did not contain calnexin. These findings indicated a successful isolation and identification of ECFC-derived exosomes (Fig. 1e-g).

3.2. Effects of THBS1-mediated ECFC-Exos on HUVEC proliferation and migration

To evaluate the ability of HUVEC to incorporate exosomes, we labeled ECFC-Exos with PKH26. Based on our confocal laser microscopy data, PKH26-labeled exosomes (red) were incorporated into the perinuclear region of HUVEC, thus confirming their internalization by HUVEC (Fig. 2a). In order to determine the optimal working concentration of exosomes, we employed the CCK8, transwell, and qRT-PCR assays to determine the impact of varying exosomes concentrations (5 μg/ml, 25 μg/ml and 50 μg/ml) on HUVEC proliferation, migration, and angiogenesis ability. Using CCK-8 assay, we observed marked increases in HUVEC proliferation in presence of ECFC-Exos ($P < 0.05$), however, there was no obvious difference between distinct exosomes concentrations ($P > 0.05$) (Fig. 2b). Based on our transcript quantification, the mRNA levels of VEGF and bFGF in HUVEC were also increased after treatment with distinct exosomes concentrations. The mRNA levels of VEGF and bFGF peaked when the exosome concentration was 25 μg/ml ($P < 0.05$) (Fig. 2c-d). Moreover, the results from the transwell assay revealed that the migration ability of HUVECs was significantly enhanced after treatment with exosomes. Moreover, when treated with 25 μg/ml exosomes concentration, the migration ability was the highest ($P < 0.05$) (Fig. 2e-f). Given these evidences, we selected the 25 μg/ml exosomes concentration for subsequent experimentations.

We next explored the significance of THBS1 in the ECFC-Exos-mediated regulation of endothelial cell proliferation and migration by knocking down THBS1 (shTHBS1-Exos) in ECFCs. We incorporated ECFCs with lentiviral vectors, and only utilized cells that obtained ≥80% transduction efficiency, verified by fluorescent microscopy. Next, we generated exosomes for the downstream assays. The inhibitory efficiency was evaluated via qRT-PCR and western blot analyses (Fig. 2h-i). Upon treatment of HUVEC with shTHBS1-Exos, CCK-8 assay revealed an enhanced ability of shTHBS1-Exos to promote HUVEC proliferation ($P < 0.05$) (Fig. 2g). As evidenced by the transwell assay, the pro-migratory effect of ECFC-Exos was also enhanced upon establishment of THBT1 deficiency in ECFC-Exos ($P < 0.05$) (Fig. 2j-k). These findings suggested that ECFC-Exo promoted endothelial cell proliferation and migration, and THBS1 played a negative regulatory role in this process.

3.3. ECFC-exo-THBS1 regulates HUVEC angiogenesis via the PI3K/Akt/ERK signaling pathway

To elucidate a potential THBS1 role in the ECFC-Exos-mediated regulation of HUVEC angiogenesis, we evaluated tube formation in these cells. Upon HUVEC treatment with shTHBS1-Exos, the cells exhibited a larger number of tube branches, compared to the Con-Exos group. The results displayed that shTHBS1-Exos displayed markedly enhanced HUVECs tube formation (Fig. 3a-b). In addition, qRT-PCR analysis revealed that the angiogenic cytokine transcript (VEGF, TGF-β, IGF) concentrations were inversely proportional to THBS1 expression in exosomes (Fig. 3c-e). These findings suggested that ECFC-Exo promoted endothelial cell angiogenesis, whereas, THBS1 suppressed endothelial angiogenesis.

The PI3K/AKT and ERK networks are well-known contributors to angiogenesis, endothelial cell migration, and proliferation. We, thus, investigated whether exosomal THBS1 regulates the PI3K/AKT/ERK pathway. To do this, we performed western blotting to detect VEGF, bFGF, PI3K, p-PI3K, AKT1, p-AKT1, ERK, and p-ERK levels in HUVEC, following treatment with shTHBS1-Exo. As shown in Fig. 3f-n, the ECFC-Exos ability to induce VEGF and bFGF expression, as well as PI3K, Akt, ERK and their phosphorylation was markedly enhanced upon THBS1 deficiency in ECFC-Exos. Taken together, our findings suggested that ECFC-Exo-THBS1 may regulate endothelial cell angiogenesis through the PI3K/Akt/ERK signaling pathway.

3.4. Exosomal THBS1 knockdown promotes DO-based angiogenesis and osteogenesis in vivo

We established a canine MDO model to explore the significance of ECFC-Exos on angiogenesis and bone remodeling in vivo (Fig. 4a). To elucidate exosome function in the distraction gap following i.v. injection, frozen tissue sections were examined under a confocal laser microscope. Red fluorescent particles were observed in the distraction gap, and some particles were enriched in the cytoplasm of cells, showing a strong

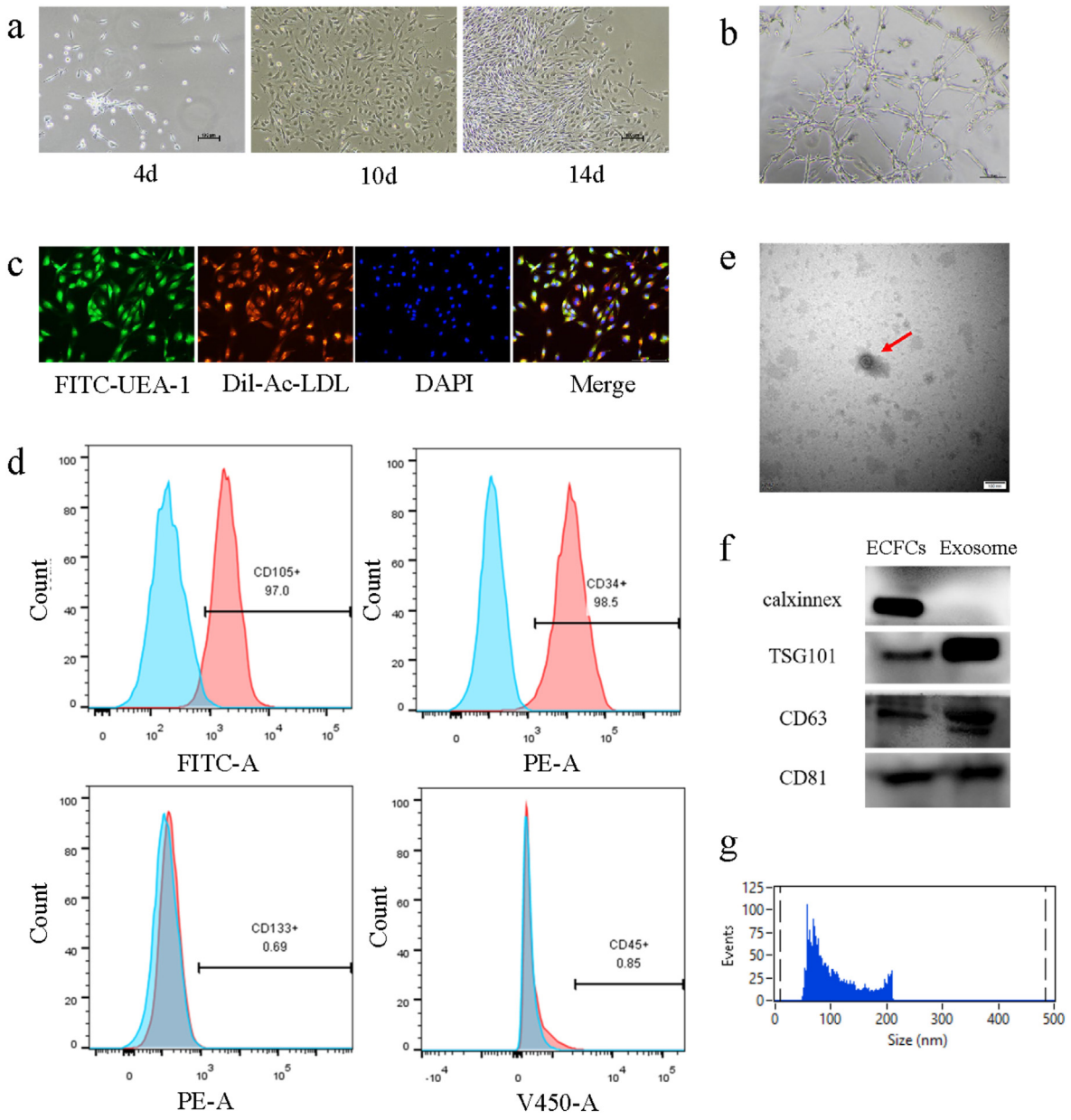

Fig. 1. Characterization of ECFCs and ECFC-Exos. (a) ECFCs morphologies on days 7, 10, and 14 of culture, exhibiting a shuttle-like morphology after 7 days in culture, and a cobblestone-like structure after 10 days (100 × , bar = 100 μm) in culture. (b) Tube forming capacity of ECFCs (100 × , bar = 100 μm). (c) ECFCs uptake of Dil-ac-LDL (red) and FITC-UEA-1 (green) (200 × , bar = 100 μm). (d) Evaluation of the ECFCs phenotypic markers by flow cytometry, CD34 and CD105 were highly positive, but CD45 and CD133 were negative. (e) The cup- or sphere-shaped ECFCs-Exos morphology, under TEM (120,000 × , bar = 100 nm). (f) ECFCs-Exos surface containing enriched proteins CD63, CD81, and TSG101, but no calnexin. (g) The nanoflow detection of particle size distribution of ECFCs-Exos. n = 3 independent experiments. (For interpretation of the references to color in this figure legend, the reader is referred to the Web version of this article.)

fluorescent aggregation (Fig. 4b). These suggested that the ECFC-Exos injected into the peripheral blood aggregated within the distraction gap, and was endocytosed into certain cells within the gap. Upon gross examination of tissues, we revealed marked differences in regional bone formation under varying treatment conditions. Moreover, according to the general observation, the shTHBS1-Exos animals exhibited active bone remodeling, with the most compact new bone formation occurring within the distraction gap, relative to animals receiving other treatments (Fig. 4c). Our radiographic analysis revealed a marked rise in the distraction gap mineralization area within the shTHBS1-Exos group, relative to other groups, and, the advantage seemed to be reflective of every time period of shTHBS1-Exos groups (Fig. 4d). Similarly, bone remodeling was assessed via Micro-CT, and the bone density (BMD values), BV/TV, Tb.Th, and Tb.N values in the canine mandibular distraction gap showed an increasing trend, with higher values observed in the shTHBS1-Exos group on DO42 (Fig. 4e-i). In contrast, the Tb.Sp in the shTHBS1-Exos group was relatively smaller, compared to other groups (Fig. 4j). These results suggested that ECFC-derived exosomal THBS1 knockdown regulated the speed and quality of DO-based osteogenesis, and this advantage was also evident in the early stages of consolidation.

Our H&E staining of the regenerated tissue revealed newly formed trabecular bone and massive neovascularization in the shTHBS1-Exos group on DO14, and, the distraction gap was replaced by a large number of newly formed trabecular bone on DO21. Compared to other groups, the distraction gap was completely replaced by new bone tissue on DO42 in the shTHBS1-Exos group, as evidenced by the mature bone Harvard system (Fig. 5a). The Masson staining also demonstrated a large

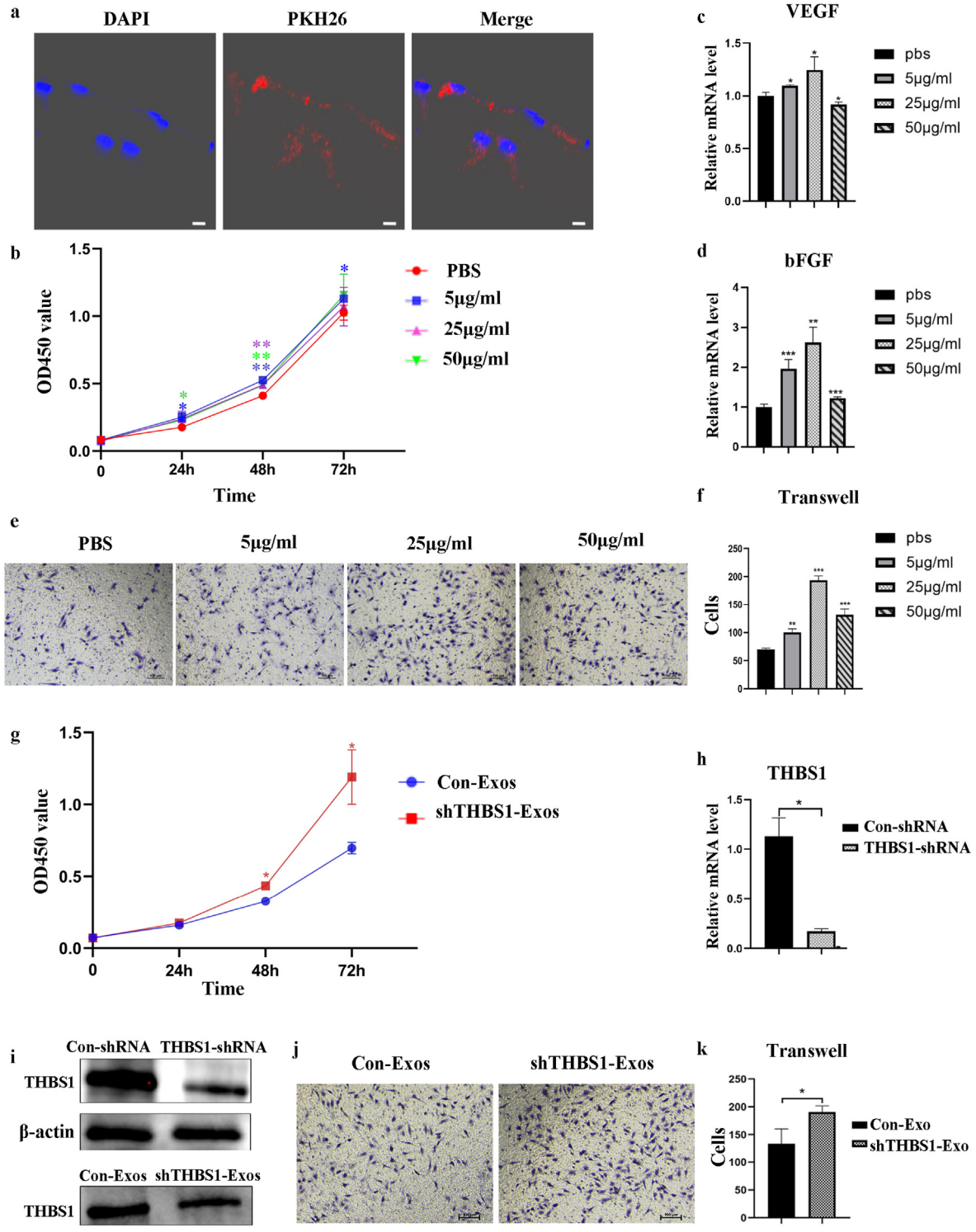

Fig. 2. The effect of ECFC-Exos THBS1-mediated regulation of HUVEC proliferation and migration. (a) PKH26-labeled (red) ECFCs-Exos incorporation by HUVECs (1000 × , bar = 10 μm). (b-f) The optimal ECFCs-Exo working concentration for CCK8, transwell, and qRT-PCR assays. b. Marked increases in HUVEC proliferation in presence of ECFC-Exos, but no difference between distinct exosomes concentrations. c-f. The HUVECs exhibited the strongest migration ability and the largest VEGF and bFGF mRNA expressions at an exosome concentration of 25 mg/ml (g) CCK-8 assay revealing an enhanced ability of shTHBS1-Exos to promote HUVEC proliferation. (h, i) The reduction of mRNA and protein THBS1 expression in ECFCs and ECFCs-Exos, following inhibition of THBS1. (j-k) Transwell assay revealing the accelerated migrating ability of HUVEC cells, after shTHBS1-Exos incorporation. *$P<0.05$, **$P<0.01$, ***$P<0.001$; n = 3 independent experiments. (For interpretation of the references to color in this figure legend, the reader is referred to the Web version of this article.)

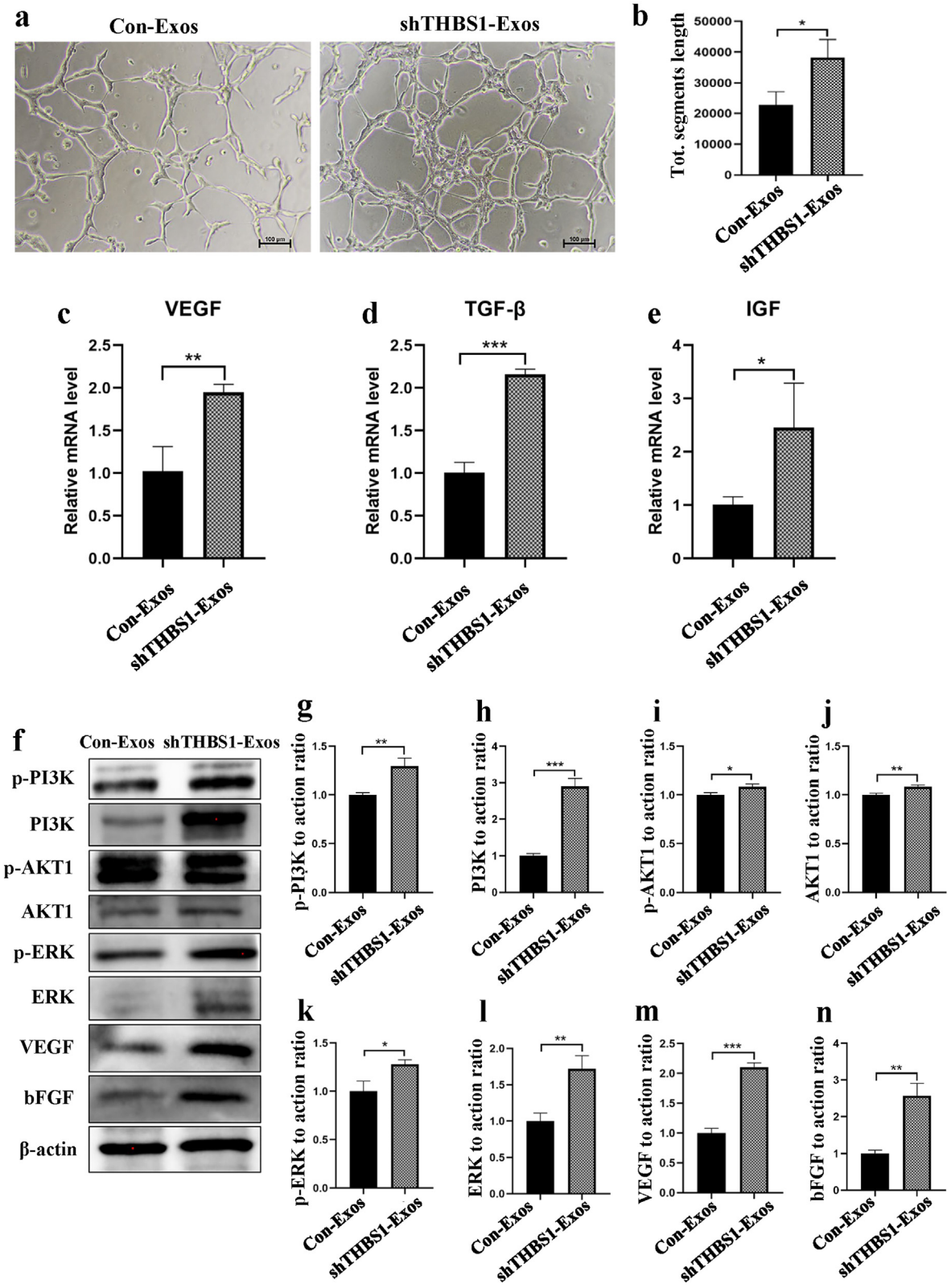

Fig. 3. ECFC-Exo-THBS1 regulates HUVEC angiogenesis via the PI3K/Akt/ERK signaling pathway. (a-b) shTHBS1-Exos promotes the tube-forming ability of HUVEC cells. (c-e) shTHBS1-Exos promotes the mRNA expression of HUVEC angiogenic factors, namely, VEGF, TGF-β, and IGF. (f-n) Western blot analyses of VEGF, bFGF, PI3K, p-PI3K, AKT1, p-AKT1, ERK, and p-ERK protein levels in HUVEC, when treated with shTHBS1-Exos. $^{*}P<0.05$, $^{**}P<0.01$, $^{***}P<0.001$; n = 3 independent experiments.

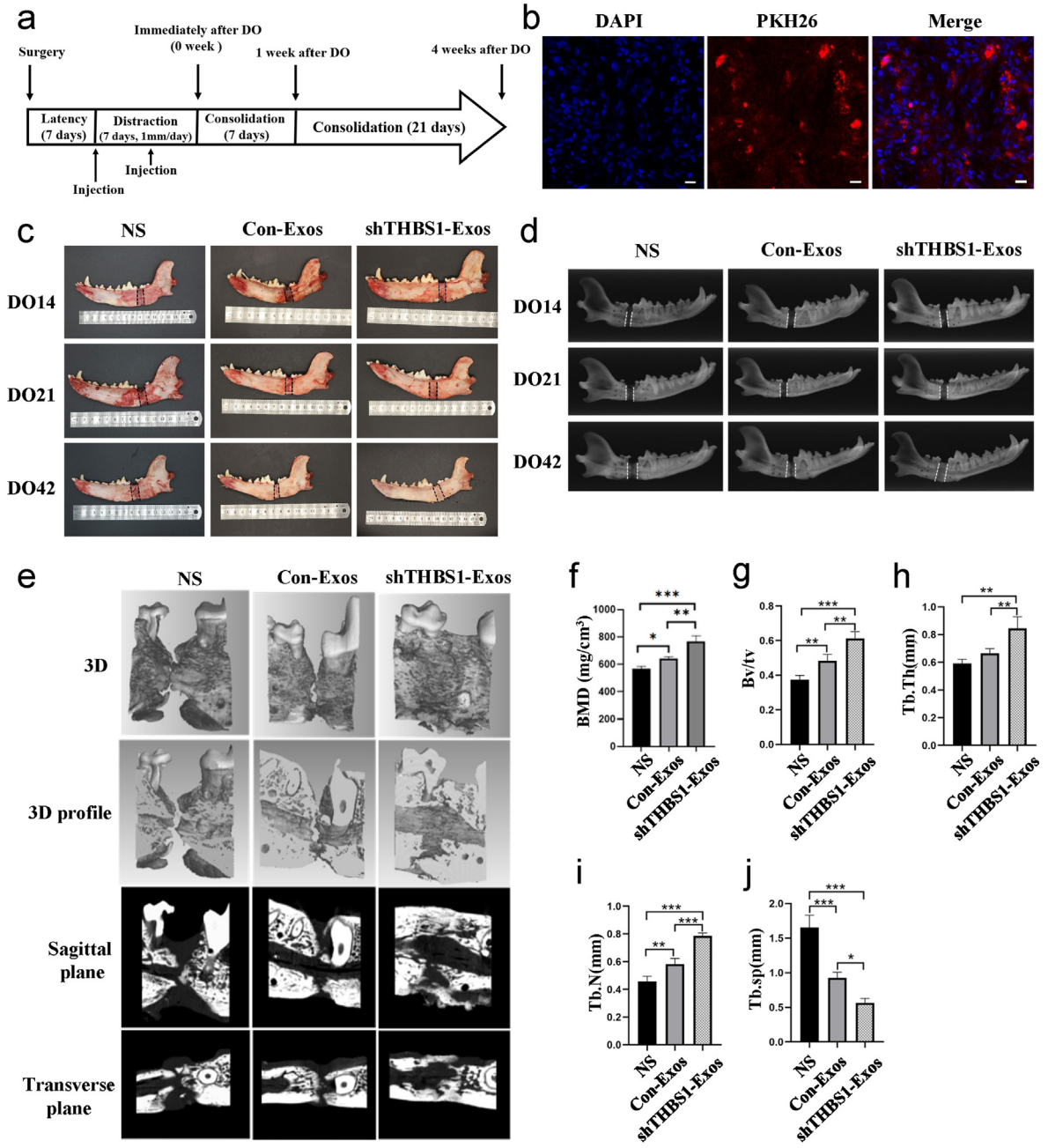

Fig. 4. Exosomal THBS1 knowndown accelerates canine mandibular distraction osteogenesis (MDO). (a) Canine model of MDO. (b) The PKH26-labeled (red) ECFC-Exos in the distraction gap (1000 × , bar = 10 μm). (c-e) Gross observation, X-ray, and three-dimensional reconstruction of the canine mandible distraction gap revealing that the shTHBS1-Exos group exhibits active bone remodeling, with the most compact new bone formation occurring within the distraction gap, as opposed to other groups. (f-i) The BMD, BV/TV, Tb.Th, and Tb.N values in the shTHBS1-Exos group exhibit significantly higher values than in other groups. (j) The Tb.Sp value in the shTHBS1-Exos group shows a drastic reduction, relative to other groups. $^{*}P<0.05$, $^{**}P<0.01$, $^{***}P<0.001$; n = 3 canine in each group, experiments were repeated thrice. (For interpretation of the references to color in this figure legend, the reader is referred to the Web version of this article.)

number of blue-stained collagen fibers, as well as immature bone trabeculae on DO14, and basically red-stained mature lamellar bone on DO42 in the shTHBS1-Exos group (Fig. 5b). Additionally, the osteogenesis and bone maturity rates of the shTHBS1-Exos group were better than in the control group. IHC CD31 staining was used to evaluate blood vessel regeneration. We demonstrated more CD31-positive vessels in the shTHBS1-Exos versus the remaining two groups, and the vessel density in the shTHBS1-Exos group was remarkably higher, relative to controls in the early consolidation phase (DO14) ($P < 0.05$) (Fig. 5c-d). To next evaluate the quality of the canine mandibular distraction gap osteogenesis, we employed IHC OCN staining. Our results revealed that osteogenesis and bone remodeling were more active in the shTHBS1-Exos group, relative to other groups (Fig. 5h). Next, we detected the transcript levels of related angiogenic genes, namely, VEGF, bFGF, and VE-cadherin in the distraction tissues on DO14, DO21 and DO42. The mRNA expression levels were the highest on DO21, and diminished on DO42. In the shTHBS1-Exos group distraction tissues, the mRNA expressions of related angiogenic genes were higher than in the control groups on DO14 and DO21, then, after fixation for 28 days, the angiogenic genes expression decreased on DO42 with an increase in bone formation (Fig. 5e-g). Collectively, our evidences suggested that exosomal THBS1 knockdown accelerated DO-based angiogenesis and osteogenesis in vivo.

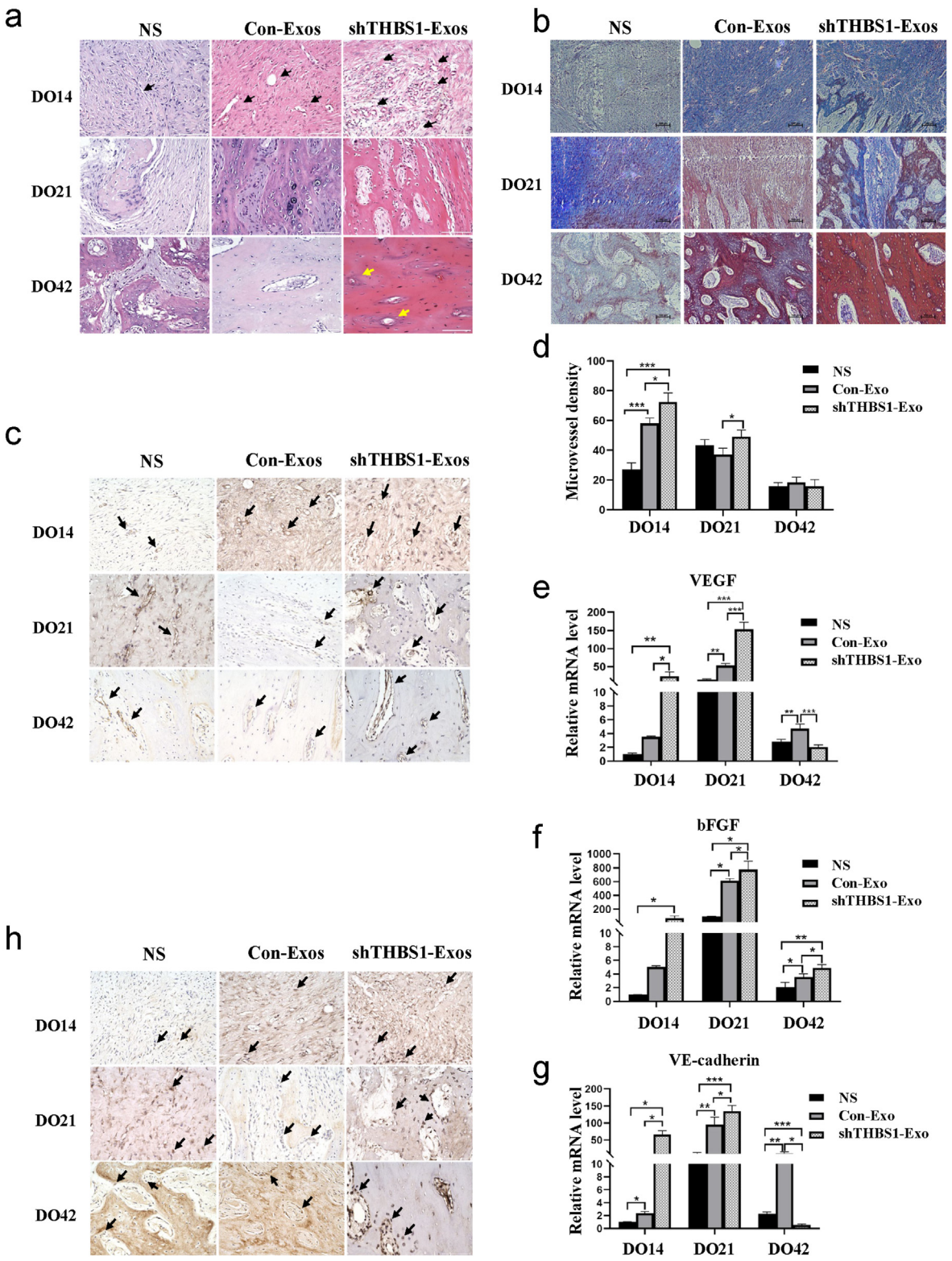

Fig. 5. Exosomal THBS1 knockdown promotes DO-based angiogenesis and osteogenesis in vivo. (a-b) The HE (400 × , bar = 100 μm, the black arrows represent new blood vessels and the yellow arrows represent the mature bone Haversian system) and Masson staining (100 × , bar = 100 μm) analyses of the regenerated tissue depicting newly formed trabecular bone, and massive neovascularization in the shTHBS1-Exos group on DO14. Compared to other groups, the distraction gap is completely replaced with new bone tissue on DO42, and the shTHBS1-Exos promotes new bone formation. (c-d) CD31 immunohistochemical (IHC) staining (400 × , bar = 100 μm, the black arrows represent new blood vessels) revealing considerably more angiogenesis and earlier peak in theshTHBS1-Exos group, as compared to other groups. (h) OCN IHC (400 × , bar = 100 μm, the black arrows represent osteoblasts) illustrating more active osteogenesis and bone remodeling in the shTHBS1-Exos group. (e-g) Marked elevation in VEGF, bFGF, and VE-cadherin transcript levels in the shTHBS1-Exos group, as opposed to other groups, in the early consolidation phase. *$P<0.05$, **$P<0.01$, ***$P<0.001$; n = 3 canine in each group, experiments were repeated in triplicate. (For interpretation of the references to color in this figure legend, the reader is referred to the Web version of this article.)

4. Discussion

Several studies reported a strong angiogenic response during DO [23,24], whereby a large amount of neovascularization occurs in the distraction gap during DO. Additionally, the regenerated tissue is often more vascularized in the DO model, as opposed to fracture healing [25]. Therefore, revealing the regulatory mechanisms of angiogenesis during DO has the potential of shortening the consolidation phase, which may, in turn, enhance therapeutic outcomes. In this study, we confirmed that ECFCs-Exos markedly enhances endothelial cells proliferation, migration, and angiogenesis in vitro. We constructed an animal model of MDO, found that THBS1 plays a crucial role in the ECFC-Exos-mediated regulation of canine MDO angiogenesis and bone remodeling.

Stem cells, genes, growth factors and other therapeutic strategies have achieved many results in the field of DO. In addition, recent studies have also reported the promoting role of biometals in DO [26]. But recent studies suggested exosomes as a promising alternative for stem cell therapy [27], which may be a better option for promoting DO. The application of exosomes in DO has unique advantages due to its improved safety, low immunogenicity, zero tumorigenic risk, easier storage, delivery, and management. Jia et al. [28] also demonstrated that exosomes secreted by young mesenchymal stem cells promote new bone formation in aged rat tibia distraction osteogenesis. Our previous investigation revealed that ECFCs are an important angiogenic mediator involved in DO [29]. It was confirmed that ECFCs-derived exosomes serve as important mediators during vascular repair and angiogenesis [30,31]. Several reports raised the possibility that ECFCs do not directly incorporate into newly developed vasculature, instead they stimulate the proliferation and migration of tissue-resident endothelial cells (ECs), using paracrine networks [32-34]. This is consistent with our findings. We confirmed that ECs incorporated ECFC-exosomes via endocytosis, which, in turn, enhanced EC proliferation, migration, and tubulogenesis. Moreover, we demonstrated that the angiogenic regulation of ECs via ECFC-exosomes was not entirely associated with concentration, and that the optimal concentration for promoting angiogenesis was 25mg/mL.

Previous studies revealed that an i.v. administration of EPC-derived exosomes directs EPC-derived exosomes to the site of vascular injury [35,36]. Jose L et al. [37] reported that in ischemia/reperfusion kidney-injured mice treated with DiR-labeled exosomes at the time of reperfusion, the peri-renal area was reduced at 30 min compared to sham mice treated with DiR-labeled exosomes. Fluorescence was significantly elevated. Their data suggest that ECFC-derived exosomes can selectively target the kidney after ischemic injury. During the distraction period of DO, the distraction zone becomes relatively ischemic and hypoxic [38]. To verify whether ECFC-Exos targets the distraction zone, we i.v. injected pKH26-labeled ECFC-Exos into an animal model of MDO, and observed the distraction region using laser confocal microscopy. Based on our observation, a large number of red fluorescence aggregated within the distraction region. This data revealed that DO not only recruited cultured and labeled EPCs to the distraction gap, but also targeted ECFC-Exos to the distraction region.

THBS1 belongs to the thrombospondin family, and was thought to be related to the angiogenic properties of ECFCs [20,22]. It is a well-recognized protein that inhibits angiogenesis, and it is expressed in multiple organisms. The PI3K/AKT network is a survival axis, which is mainly involved in physiological processes, such as, cell survival, metabolic regulation, endocytosis, and anti-apoptosis [39]. Additionally, it is related to the formation of blood vessels, as well as migration, and proliferation of endothelial cells [40]. THBS1 can alter expression of PI3K and Akt [41]. THBS1 overexpression is known to cause PI3K inhibition, which, in turn, abrogates the VEGF/Akt/PI3K cascade, thereby preventing angiogenesis and endothelial cell proliferation [42,43]. This is consistent with our results which showed that THBS1 inhibition in ECFCs-Exo induced enhanced phosphorylation of PI3K, AKT, and ERK in endothelial cells, thereby enhancing expressions of angiogenesis-related factors VEGF and bFGF. Our current findings suggested that THBS1 was a key mediator of ECFCs-Exo-mediated HUVEC angiogenic regulation. Next, we speculated that the ECFCs-Exo activates the PI3K/AKT/ERK signaling pathway by downregulating THBS1. Additionally, this action positively regulates HUVEC proliferation, migration, and angiogenesis, and promotes angiogenic factor expressions. Based on our observations, we found that THBS1 in ECFC-Exos negatively regulated endothelial cell angiogenesis, as demonstrated by migration, tube formation, and PCR assays in vitro. In contract, THBS1 deficient exosomes promoted angiogenesis of endothelial cells.

Furthermore, in this study, we assumed that ECFCs-derived exosomes regulate the speed and quality of angiogenesis via THBS1, thereby shortening the DO consolidation phase. To verify our hypothesis, we assessed the pro-angiogenic and osteogenic abilities of ECFCs-Exo in the MDO beagle model in vivo. We suppressed THBS1 expression in ECFCs, extracted ECFCs-Exo, and injected into the MDO animal models. Based on our Micro-CT evaluation, THBS1 suppression significantly increased osteogenic mass and velocity of the distraction callus. Previous studies confirmed that an intense angiogenic activity was observed during the distraction phase and the early consolidation phase [44,45]. Our H&E and Masson staining results found that the THBS1 inhibition in ECFCs-Exo promoted angiogenesis in the canine mandibular distraction callus, and, simultaneously, significantly enhanced the rate of bone formation and bone maturation, as confirmed via IHC. The in vivo results support that the beneficial effects of ECFCs-Exo on osteogenesis during DO may be attributed to enhanced angiogenesis, and that THBS1 is responsible key medium for ECFCs-Exo promoting angiogenesis and bone formation in DO callus.

Collectively, our data suggested that THBS1 suppression in ECFCs-Exo accelerated angiogenesis in the mandibular DO callus, which, in turn, accelerated bone remodeling. However, since exosomes contain various bioactive components, including proteins, lipids, and RNAs, the therapeutic effects of ECFCs-Exo may be mediated through multiple mechanisms. Moreover, due to costs and technical limitations, it was still a challenge to isolate large quantities of specific exosomes. Hence, how to fully apply the potential of exosomes to clinical treatment still needs a lot of research and exploration.

5. Conclusion

Notably, we were the first to identify that THBS1 plays a crucial role in the ECFC-Exos-mediated regulation of canine MDO angiogenesis and bone remodeling. Based on our analyses, THBS1 suppression in ECFC-Exos activated the PI3K/AKT/ERK network, which, in turn, promoted HUVEC proliferation, migration, and angiogenesis. Hence, the angiogenic promotion via THBS1 suppression in ECFC-Exos may be a promising strategy for shortening the DO duration.

Ethical approval statement

All animal studies described herein were reviewed and approved by the Animal Care and Use Committee of Guangxi Medical University (No. 202012014).

Funding/support statement

This work was supported by the National Natural Science Foundation of China under Grant (82071098); Guangxi Medical University Youth Science Foundation (GXMUYSF202228); Guangxi high-level medical talent training plan (’139’ plan) (G201901005); Guangxi Science and Technology Base and Talents Special Project (2021AC18031); Guangxi Medical and health suitable technology development and popularization applications project (S2021085).

Author contributions

Xuanping Huang and Nuo Zhou designed the study; Fengchun Liao

and Tao Zhang obtained the data; Fengchun Liao, Tao Zhang, and Weidong Jiang performed the animal experiments; Peiqi Zhu, Zhenchen Zhao, Henglei Shi, and Dan Zhao performed in vitro studies; Fengchun Liao and Ziqi Liao assisted in data analysis and wrote the manuscript; Xuanping Huang and Nuo Zhou revised the manuscript and final approved the manuscript submission.

Declaration of competing interest

None.

Acknowledgements

The authors would like to thank all the reviewers who participated in the review, as well as MJEditor (www.mjeditor.com) for providing English editing services during the preparation of this manuscript.

References

[1] Annino Jr DJ, Goguen LA, Karmody CS. Distraction osteogenesis for reconstruction of mandibular symphyseal defects. Arch Otolaryngol Head Neck Surg 1994;120(9):911–6.
[2] Fang TD, Salim A, Xia W, Nacamuli RP, Guccione S, Song HM, et al. Angiogenesis is required for successful bone induction during distraction osteogenesis. J Bone Miner Res 2005;20(7):1114–24.
[3] Kang F, Yi Q, Gu P, Dong Y, Zhang Z, Zhang L, et al. Controlled growth factor delivery system with osteogenic-angiogenic coupling effect for bone regeneration. J Orthop Translat 2021;31:110–25.
[4] Sivaraj KK, Adams RH. Blood vessel formation and function in bone. Development 2016;143(15):2706–15.
[5] Lee DY, Cho TJ, Kim JA, Lee HR, Yoo WJ, Chung CY, et al. Mobilization of endothelial progenitor cells in fracture healing and distraction osteogenesis. Bone 2008;42(5):932–41.
[6] Lee DY, Cho TJ, Lee HR, Park MS, Yoo WJ, Chung CY, et al. Distraction osteogenesis induces endothelial progenitor cell mobilization without inflammatory response in man. Bone 2010;46(3):673–9.
[7] Vinas JL, Burger D, Zimpelmann J, Haneef R, Knoll W, Campbell P, et al. Transfer of microRNA-486-5p from human endothelial colony forming cell-derived exosomes reduces ischemic kidney injury. Kidney Int 2016;90(6):1238–50.
[8] Faris P, Negri S, Perna A, Rosti V, Guerra G, Moccia F. Therapeutic potential of endothelial colony-forming cells in ischemic disease: strategies to improve their regenerative efficacy. Int J Mol Sci 2020;21(19).
[9] Sokolova V, Ludwig AK, Hornung S, Rotan O, Horn PA, Epple M, et al. Characterisation of exosomes derived from human cells by nanoparticle tracking analysis and scanning electron microscopy. Colloids Surf B Biointerfaces 2011;87(1):146–50.
[10] van Niel G, D'Angelo G, Raposo G. Shedding light on the cell biology of extracellular vesicles. Nat Rev Mol Cell Biol 2018;19(4):213–28.
[11] Pan D, Liu W, Zhu S, Fan B, Yu N, Ning G, et al. Potential of different cells-derived exosomal microRNA cargos for treating spinal cord injury. J Orthop Translat 2021;31:33–40.
[12] Yan L, Liu G, Wu X. Exosomes derived from umbilical cord mesenchymal stem cells in mechanical environment show improved osteochondral activity via upregulation of LncRNA H19. J Orthop Translat 2021;26:111–20.
[13] Ren K. Exosomes in perspective: a potential surrogate for stem cell therapy. Odontology 2019;107(3):271–84.
[14] Zhu S, Yao F, Qiu H, Zhang G, Xu H, Xu J. Coupling factors and exosomal packaging microRNAs involved in the regulation of bone remodelling. Biol Rev Camb Phil Soc 2018;93(1):469–80.
[15] Zhang Y, Hao Z, Wang P, Xia Y, Wu J, Xia D, et al. Exosomes from human umbilical cord mesenchymal stem cells enhance fracture healing through HIF-1alpha-mediated promotion of angiogenesis in a rat model of stabilized fracture. Cell Prolif 2019;52(2):e12570.
[16] Taraboletti G, Roberts D, Liotta LA, Giavazzi R. Platelet thrombospondin modulates endothelial cell adhesion, motility, and growth: a potential angiogenesis regulatory factor. J Cell Biol 1990;111(2):765–72.
[17] Short SM, Derrien A, Narsimhan RP, Lawler J, Ingber DE, Zetter BR. Inhibition of endothelial cell migration by thrombospondin-1 type-1 repeats is mediated by beta1 integrins. J Cell Biol 2005;168(4):643–53.
[18] Takahashi K, Sumarriva K, Kim R, Jiang R, Brantley-Sieders DM, Chen J, et al. Determination of the cd148-interacting region in thrombospondin-1. PLoS One 2016;11(5):e0154916.
[19] Dias JV, Benslimane-Ahmim Z, Egot M, Lokajczyk A, Grelac F, Galy-Fauroux I, et al. A motif within the N-terminal domain of TSP-1 specifically promotes the proangiogenic activity of endothelial colony-forming cells. Biochem Pharmacol 2012;84(8):1014–23.
[20] Ligi I, Simoncini S, Tellier E, Vassallo PF, Sabatier F, Guillet B, et al. A switch toward angiostatic gene expression impairs the angiogenic properties of endothelial progenitor cells in low birth weight preterm infants. Blood 2011;118(6):1699–709.
[21] Hu H, Wang B, Jiang C, Li R, Zhao J. Endothelial progenitor cell-derived exosomes facilitate vascular endothelial cell repair through shuttling miR-21-5p to modulate Thrombospondin-1 expression. Clin Sci (Lond) 2019;133(14):1629–44.
[22] Eslava-Alcon S, Extremera-Garcia MJ, Sanchez-Gomar I, Beltran-Camacho L, Rosal-Vela A, Munoz J, et al. Atherosclerotic pre-conditioning affects the paracrine role of circulating angiogenic cells ex-vivo. Int J Mol Sci 2020;21(15).
[23] Li G, Simpson AH, Kenwright J, Triffitt JT. Effect of lengthening rate on angiogenesis during distraction osteogenesis. J Orthop Res 1999;17(3):362–7.
[24] Carvalho RS, Einhorn TA, Lehmann W, Edgar C, Al-Yamani A, Apazidis A, et al. The role of angiogenesis in a murine tibial model of distraction osteogenesis. Bone 2004;34(5):849–61.
[25] Jazrawi LM, Majeska RJ, Klein ML, Kagel E, Stromberg L, Einhorn TA. Bone and cartilage formation in an experimental model of distraction osteogenesis. J Orthop Trauma 1998;12(2):111–6.
[26] Li Y, Pan Q, Xu J, He X, Li HA, Oldridge DA, et al. Overview of methods for enhancing bone regeneration in distraction osteogenesis: potential roles of biometals. J Orthop Translat 2021;27:110–8.
[27] Jing H, He X, Zheng J. Exosomes and regenerative medicine: state of the art and perspectives. Transl Res 2018;196:1–16.
[28] Jia Y, Qiu S, Xu J, Kang Q, Chai Y. Exosomes secreted by young mesenchymal stem cells promote new bone formation during distraction osteogenesis in older rats. Calcif Tissue Int 2020;106(5):509–17.
[29] Jiang W, Zhu P, Zhang T, Liao F, Yu Y, Liu Y, et al. MicroRNA-205 mediates endothelial progenitor functions in distraction osteogenesis by targeting the transcription regulator NOTCH2. Stem Cell Res Ther 2021;12(1):101.
[30] Ke X, Liao Z, Luo X, Chen JQ, Deng M, Huang Y, et al. Endothelial colony-forming cell-derived exosomal miR-21-5p regulates autophagic flux to promote vascular endothelial repair by inhibiting SIPL1A2 in atherosclerosis. Cell Commun Signal 2022;20(1):30.
[31] Gao W, Li F, Liu L, Xu X, Zhang B, Wu Y, et al. Endothelial colony-forming cell-derived exosomes restore blood-brain barrier continuity in mice subjected to traumatic brain injury. Exp Neurol 2018;307:99–108.
[32] Burger D, Vinas JL, Akbari S, Dehak H, Knoll W, Gutsol A, et al. Human endothelial colony-forming cells protect against acute kidney injury: role of exosomes. Am J Pathol 2015;185(8):2309–23.
[33] Li X, Chen C, Wei L, Li Q, Niu X, Xu Y, et al. Exosomes derived from endothelial progenitor cells attenuate vascular repair and accelerate reendothelialization by enhancing endothelial function. Cytotherapy 2016;18(2):253–62.
[34] Zhang J, Chen C, Hu B, Niu X, Liu X, Zhang G, et al. Exosomes derived from human endothelial progenitor cells accelerate cutaneous wound healing by promoting angiogenesis through erk1/2 signaling. Int J Biol Sci 2016;12(12):1472–87.
[35] Kong J, Wang F, Zhang J, Cui Y, Pan L, Zhang W, et al. Exosomes of endothelial progenitor cells inhibit neointima formation after carotid artery injury. J Surg Res 2018;232:398–407.
[36] Wu X, Liu Z, Hu L, Gu W, Zhu L. Exosomes derived from endothelial progenitor cells ameliorate acute lung injury by transferring miR-126. Exp Cell Res 2018;370(1):13–23.
[37] Vinas JL, Spence M, Gutsol A, Knoll W, Burger D, Zimpelmann J, et al. Receptor-ligand interaction mediates targeting of endothelial colony forming cell-derived exosomes to the kidney after ischemic injury. Sci Rep 2018;8(1):16320.
[38] Lee DY, Cho TJ, Kim JA, Lee HR, Yoo WJ, Chung CY, et al. Mobilization of endothelial progenitor cells in fracture healing and distraction osteogenesis. Bone 2008;42(5):932–41.
[39] Henson ES, Gibson SB. Surviving cell death through epidermal growth factor (EGF) signal transduction pathways: implications for cancer therapy. Cell Signal 2006;18(12):2089–97.
[40] Chen Z, Liu G, Xiao Y, Lu P. Adrenomedullin22-52 suppresses high-glucose-induced migration, proliferation, and tube formation of human retinal endothelial cells. Mol Vis 2014;20:259–69.
[41] Huang T, Wang L, Liu D, Li P, Xiong H, Zhuang L, et al. FGF7/FGFR2 signal promotes invasion and migration in human gastric cancer through upregulation of thrombospondin-1. Int J Oncol 2017;50(5):1501–12.
[42] Li S, Li H, Xu Y, Lv X. Identification of candidate biomarkers for epithelial ovarian cancer metastasis using microarray data. Oncol Lett 2017;14(4):3967–74.
[43] Ma Y, Dong C, Chen X, Zhu R, Wang J. Silencing of miR-20b-5p exerts inhibitory effect on diabetic retinopathy via inactivation of THBS1 gene induced VEGF/Akt/PI3K pathway. Diabetes Metab Syndr Obes 2021;14:1183–93.
[44] Rowe NM, Mehrara BJ, Luchs JS, Dudziak ME, Steinbrech DS, Illei PB, et al. Angiogenesis during mandibular distraction osteogenesis. Ann Plast Surg 1999;42(5):470–5.
[45] Byun JH, Park BW, Kim JR, Lee JH. Expression of vascular endothelial growth factor and its receptors after mandibular distraction osteogenesis. Int J Oral Maxillofac Surg 2007;36(4):338–44.